Paleobiology, 19(1), 1993, pp. 71–91

A model for planktic foraminiferal shell growth

Miguel Signes, Jelle Bijma, Christoph Hemleben, and Rolf Ott

Abstract.—In this paper we analyze the laws of growth that control planktic foraminiferal shell morphology. We assume that isometry is the key toward the understanding of their ontogeny. Hence, our null hypothesis is that these organisms construct isometric shells. To test this hypothesis, geometric models of their shells have been generated with a personal computer. It is demonstrated that early chambers in log-spirally coiled structures cannot follow a strict isometric arrangement. In the real world, the centers of juvenile chambers deviate from the logarithmic growth curve. Juvenile stages are generally more planispiral and contain more chambers per whorl than adult stages. These traits are shown to be essential in order to keep volumes of consecutive chambers in geometric progression. We are convinced that the neanic stage marks the constructional bridge from a juvenile set of growth parameters to an adult one. The adult stage can be strictly isometric, that is, the effective shape is constant and the increase in volume after a chamber addition is proportional to the preexisting volume of the shell.

The shell volume is related to the biomass, the ratio of outer shell surface area to shell volume is related to the respiration rate and the ratio of the total shell surface area to shell volume is related to the total calcification effort. The influence of the parameters of the model on these relationships is investigated. Only the initial radius and the rate of radius increase affect the relationships between shell volume and surface area. The other shape parameters merely provide a fine tune-up of these relationships. Size itself plays a major role during foraminiferal development.

Miguel Signes. Departamento de Geología, Facultat de Ciencias Biológicas, Universitat de València, 46100-Burjassot, Spain

Jelle Bijma, Christoph Hemleben, and Rolf Ott. Geologisches-Paläontologisches Institut, Universität Tübingen, Sigwartstrasse 10, 7400-Tübingen, West Germany

Accepted: May 26, 1992

Introduction

In paleontology, three quantitative approaches toward the analysis of the shape of biological structures are commonly used. The first approach includes methods like Fourier shape analysis, Eigenshape analysis, and other statistical techniques to describe planar projections of the outline in terms of a reduced set of variables (e.g., harmonics, eigenshapes, principal components). After selection and description of the variables, correlations with environmental parameters can be established. Among others, Healy-Williams and Williams (1981) and Lohmann (1983) applied this method to describe planktic foraminiferal test shape. This procedure has a strong descriptive potential but often contributes little to the explanation of shapes. The second approach is based on the extraction of geometric features from constellations of homologous landmarks (Bookstein et al. 1985; Bookstein 1986; Rohlf and Bookstein 1990). This method requires no a priori assumptions of the true morphogenic features because the variation or differences in the data set determine the morphological features. The landmark approach has also been used for morphometric studies on planktic foraminifers (Macleod and Kitchell 1990; Tabachnick and Bookstein 1990a,b). This approach pretends to have a stronger explanatory power than the first one.

The third approach is model-based and makes use of the methods of functional, theoretical, and constructional morphology in order to establish relationships between factors that give rise to organic shape (e.g., Gould 1970; Seilacher 1970). Expansions of the three original factors of the constructional morphology (Raup 1972; Hickman 1980; De Renzi 1982) and contributions from the science of development and evolutionary theory (Waddington 1968; Bonner 1982) are the theoretical framework for the geometrical model

0094-8373/93/1901-0005/$1.00

presented herein. The model simulates the basic morphology (chamber size and spatial arrangement) of some planktic foraminiferal shells. The model is intended to study functional properties of the different morphologies rather than to describe shapes in terms of a set of parameters. Although the second approach supercedes model building in some respects (Rohlf 1990), the simultaneous description of shape and the estimation of volume and surface area require a model-based approach. Volume and surface area are thought to have an important impact on shape and vice versa. The model presented herein belongs to a family of so-called "fixed-axis" coiling models (see, e.g., Moseley 1938; Thompson 1942; Raup and Michelson 1965; Raup 1966; Berger 1969). However, the axis of coiling may not be stable (e.g., streptospiral coiling in *Pulleniatina obliquiloculata* [Parker and Jones] or heteromorphic ammonites) and often lacks a physical representation on shells. More recently, models have been introduced that describe accretionary growth independent of an "axis of coiling" (Okamoto 1988; Ackerly 1989). The advantage of these local-coordinate models is that they describe growth from an organismal vantage point, that is, from the aperture. The perception of a unique coiling axis may be an antropogenic interpretation of spiral growth. However, it is difficult to estimate the orientations of apertural planes in all but the most simply coiled forms. Therefore we choose to use a fixed coiling axis as a landmark.

Although there are no objections against allometric growth, there are good arguments to base the model on the principle of geometric similitude. Quantitative support for the assumption that planktic foraminifera grow according to the laws of isometry comes from indirect evidence. Isometric growth, or the principle of geometric similitude, is the only reasonable way to explain log-spiral patterns of shell coiling (Thompson 1942; Berger 1969; Scott 1970, 1972, 1973; Olsson 1971, 1972, 1973). Properties that are characteristic of log-spirally coiling shells, such as a constant ratio between the diameters of consecutive chambers, have been reported for some planktic foraminifers (see, e.g., Scott 1974 and references therein). The phase transitions during planktic foraminiferal ontogeny correlate with size rather than with a specific number of chambers (Brummer et al. 1986, 1987; Huber 1987, MS; Wei MS). These observations suggest that a rather simple *Bauplan* underlies foraminiferal architecture (see Norris 1991) and provides support for the assumption that the laws of construction are oriented toward isometric shell morphologies.

Additional support may come from considerations about the evolution of the group as a whole. Planktic foraminiferal phylogeny is characterized by two major periods of adaptive radiation, one at the Late-Early Cretaceous and one after the Cretaceous-Tertiary boundary (see, e.g., Cifelli 1969; Hart 1980; Tappan and Loeblich 1988). A minor period of adaptive radiation starts after the Paleogene-Neogene boundary, where the number of species is markedly reduced. In periods of radiation, the ancestral groups are small and bear less shell complexity relative to their descendants (Stanley 1973; Gould 1988). The development from small to large has often been used to demonstrate the adaptive significance of allometry in ontogeny and phylogeny (see, e.g., Gould 1966, 1968). In the absence of allometry, the ratio of surface area to volume must decline as size increases. However, the collective increase of shell size and diversity could also be explained in favor of isometry. The ancestors in each radiation are small because isometric growth in general brings along scaling problems that often determine an upper limit for size. Only after solutions to these problems were "invented," could size increase. Many such problems have their roots in the disparate increase of body volume and surface area with size (see, e.g., Gould 1966, 1968). The analysis of the relationships between these features and shape are of primary importance for understanding planktic foraminiferal shell architecture. Properties like biomass, shell weight, calcification effort, and respiration rate are derived from the first two. In this paper we consider the relationships between size and shape to be of primary importance for understanding planktic foraminiferal shell architecture. The effects of varying chamber arrangement and their relative

dimensions on shell volume and surface area are quantitatively investigated.

In order to study some properties of foraminiferal shells, we have designed a simulation model that accounts for size and arrangement of spherical subunits in a three-dimensional space. The model has been implemented in a computer program (REMAKER), written in PASCAL and run on an MS-DOS personal computer. The structures generated with the program are isometric and resemble foraminiferal shells. Strictly speaking we should refer to "geometric structures consisting of overlapping subunits" but for a better understanding and because we simulate foraminiferal growth we refer to "shells made up of chambers."

Assumptions of the Model

The structures, determined by the model, are isometric provided the following two conditions are met: (1) the shape of the subunits (chambers) is constant; and (2) the increase in volume after the addition of a new subunit is proportional to the preexisting volume of the structure.

The first condition restricts the application of the model to those shells, or ontogenetic stages, where chamber shape is constant (structurally stable in the sense of Thom 1977). The second condition refers to exponential growth per stage. It is convenient to distinguish shell-size increase from cytoplasmic growth because the first is discontinuous and the second is continuous. In figure 1A, the cytoplasmic size was derived using Gompertz's model (Lebreton and Milier 1982) and shell growth according to the second condition of the model. Exponential, chamber-by-chamber, shell size increase does not necessarily imply an exponential function between growth of the cytoplasm and time. The latter usually follows a logistic pattern rather than an exponential one (fig. 1A). As a consequence of this uncoupling, a direct relationship between shell volume and biomass can be established only at the events of chamber formation.

An exponential increase in shell size suggests an exponential increase in biomass from one stage to the next (i.e., exponential growth per stage). Some clues sustain the assumption of exponential biomass increase per chamber increment in planktic foraminifers. If any small portion of cytoplasm has the ability to grow to a certain degree and all those portions grow within a certain time, then the biomass increases exponentially. An idealized representation of the relationships between shell growth and cytoplasmic growth is shown in figure 1A.

Although the sequence of developmental events cannot be referred to an absolute time scale, it is useful to describe the relationship

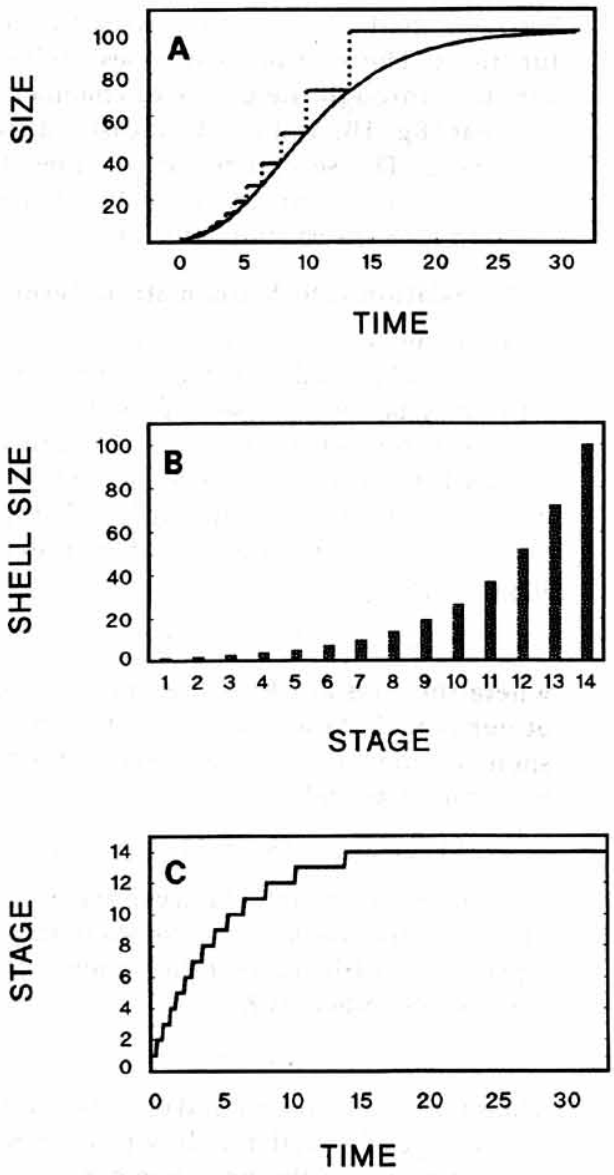

FIGURE 1. A, Idealized representation of protoplasmic growth (continuous line) and shell growth (stepped line). B, Shell growth per stage. C, Rate of chamber formation. Size in arbitrary units, and time in days.

between shell size and time with two step functions. The first one expresses shell-size variation through the course of chamber increment (fig. 1B) and can be measured from specimens. The second relates chamber formation to time and can only be obtained through live observations (fig. 1C).

Translation into Mathematical Terms

From the second condition of the model (exponential growth per stage), several properties may be derived (see Appendix A for a full derivation of the relationships and Appendix B for a list of parameters and abbreviations). Chamber volume (CV) is proportional to the shell volume (SV) at the previous stage of growth,

$$CV_{n+1} = KtSV_n \qquad n \geq 1, \tag{1}$$

where the constant Kt is the first parameter of our model. As a result, the ratio between shell volumes at two consecutive stages must be constant as well:

$$SV_{n+1}/SV_n = (Kt + 1) \qquad n \geq 1. \tag{2a}$$

Consequently, the ratio between the volumes of consecutive chambers is constant and also equals $Kt + 1$ (the ratio of the volumes of the first two chambers is Kt):

$$CV_{n+1}/CV_n = (Kt + 1) \qquad n \geq 1. \tag{2b}$$

Therefore, shell volume and chamber volume at any stage of growth may be written in terms of the volume of the first chamber:

$$SV_n = CV_1(Kt + 1)^{n-1} \qquad n \geq 1 \tag{3a}$$

$$CV_n = CV_1Kt(Kt + 1)^{n-2} \qquad n \geq 1. \tag{3b}$$

The above relationships and properties apply to any isometric structure, regardless of the shape of the chambers. The scope of the model is purported to simulate shell growth where consecutive chambers are contiguous and arranged in an orderly manner. Thus, there exist only three possible kinds of chamber arrangements: (1) linear (uniserial), (2) completely involute, and (3) log-spiral (including multiserial forms).

At this point, it is convenient to distinguish between the *basic shape* and the *effective shape* of the chambers. The basic shape of a chamber is a sphere, but the effective shape is a sphere missing one or more sections because of overlaps with earlier chambers. In isometric growth, the basic chamber shape and the effective chamber shape must be constant.

In log-spiral arrangement, the configuration of most planktic foraminiferal shells, the effective shapes of early chambers vary following changing overlap patterns. The second chamber overlaps only with the first, whereas the third overlaps with the second and possibly with the first, and so on until a constant pattern of overlap is reached (fig. 2). The chamber at which the effective shapes become constant is defined as the first regular chamber (FRC). From there onward, the chambers have exactly the same pattern of overlap and thus the same effective shape. In shells with linear or involute chamber arrangements, the first regular chamber is the second chamber. In log-spiral shells, the first regular chamber is usually not reached before the second whorl.

Provided that the basic shape of the chambers is a sphere, the volume of the nth chamber may be expressed as

$$CV_n = (4\pi/3)R_n^3\delta_n, \tag{4}$$

where R is the radius of the basic chamber shape, and δ is the ratio between the volume of the effective chamber and the basic chamber. By combining equations (3b) and (4), a general expression for the radius of any chamber is obtained:

$$R_n^3 = Kt(Kt + 1)^{n-2} R_p^3/\delta_n, \tag{5}$$

where R_p is the radius of the first chamber. Consequently, the ratio between radii of consecutive chambers is constant when δ does not change (from one chamber to the next). In early chambers, the loss of volume with respect to a corresponding sphere increases because of the increasing overlaps. Consequently, δ_n decreases from the second chamber toward the first regular chamber. From that chamber onward, δ is constant. In general,

$$(R_{n+1}^3\delta_{n+1})/(R_n^3\delta_n) = Kt + 1. \tag{6}$$

Because the size of the first chamber is significant with respect to that of the following

chambers, the difference in the relative losses of volume with respect to their original spheres is also considerable. Consequently, if the chamber radii are in geometric progression, the ratios between their volumes are not in agreement with the second condition of the model before the first regular chamber. In order to maintain exponential growth per chamber increment, it is necessary to compensate for these losses of volume in the chambers before the first regular chamber. Apart from changing chamber shape, two solutions are of special interest to bring either size or position of the chambers before the first regular chamber in agreement with the second condition of the model.

First, if all chambers are strictly arranged according to a logarithmic spiral, δ_n decreases from the second chamber to the first regular chamber. To maintain exponential growth per chamber increment, the ratio of successive radii must increase from the second chamber onward (see eq. 6). From the first regular chamber onward, this ratio stabilizes at $(Kt + 1)^{1/3}$. Thus, the ratio between the radii of consecutive chambers is larger in chambers before the first regular chamber than in later ones.

Second, if early chambers deviate from log-spiral coiling, their new positions may be such that the volumes of the consecutive chambers remain in geometric progression. Consequently, δ is constant from the second chamber onward and equals $(Kt + 1)^{1/3}$ $(=\delta_{FRC})$. To keep the volumes of consecutive chambers in geometric progression before the first regular chamber, the following solutions are possible: (1) a more planispiral shell before the first regular chamber and a more trochospiral shell after the first regular chamber; (2) a decreasing number of chambers per whorl toward the first regular chamber, and a constant number of chambers per whorl from the first regular chamber onward; or (3) a larger umbilicus before the first regular chamber than thereafter. Each of these features or combinations thereof are characteristic for early ontogenetic shell development in some recent and fossil planktic foraminifers (Brummer et al. 1986, 1987; Huber MS; Wei MS). From the first regular chamber onward, the size and position of the chambers are compatible with the second condition of the model; that is, the rate of radius increase is constant and the centers of the chambers are log-spirally arranged.

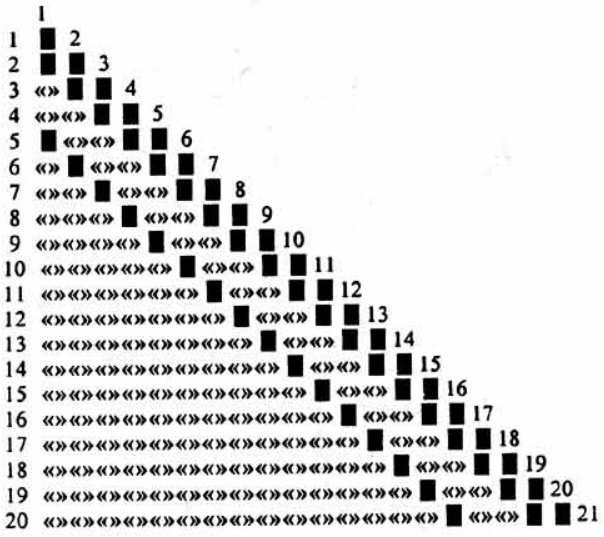

FIGURE 2. Diagram indicating the pattern of overlap between the chambers of the structure of figure 5B and 5E. Solid bar, the two chambers of the corresponding row and column overlap each other.

Size of the Chambers.—Four parameters and two scaling factors suffice to determine fully the size and position of the chambers in the shells. Although equation (5) provides a method to calculate the size of any chamber in the structure, the factor δ_n complicates a straightforward application. Assuming that all radii are in geometric progression, as seems to be the case in planktic foraminifers,

$$R_n^3 = (Kt + 1)^{n-1} R_p^3. \qquad (7)$$

Equation (7) will turn out to be in disagreement with equation (5). However, according to equation (6), equations (5) and (7) are in agreement after the first regular chamber. For chambers following the first regular chamber, equation (5) may then be rewritten as

$$R_n^3 = Kt(Kt + 1)^{n-2} R_1^3/\delta_{FRC}. \qquad (8)$$

Although both R_p and R_1 represent the radius of the initial chamber in equations (7) and (8), they are fundamentally different. R_p is merely a scaling factor for the computer to calculate the following radii. R_1, on the other hand, is a measure of the size of the first

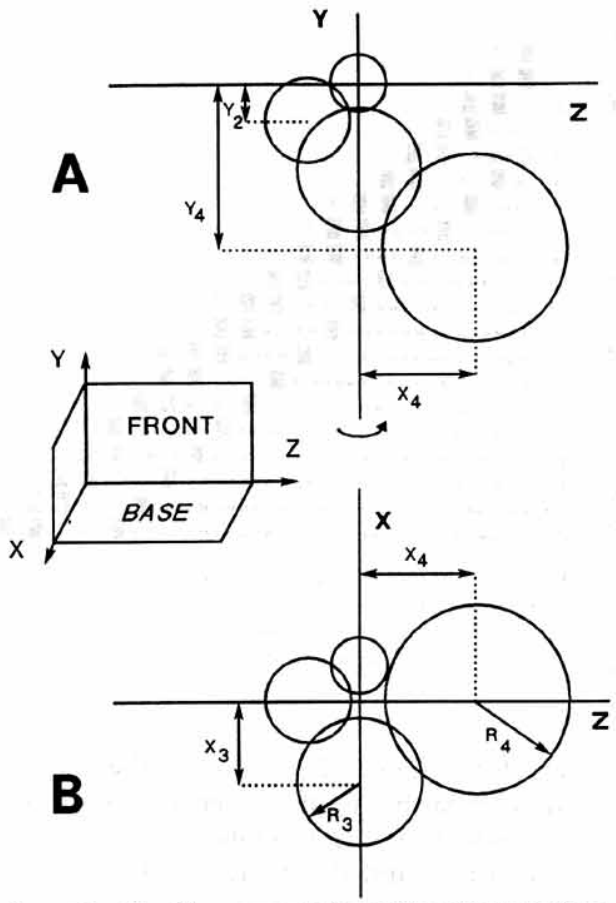

FIGURE 3. Graphic representations of the structures (four chambers per whorl ($\phi = \pi/2$)) as projections over three perpendicular planes (front, base and side). The y axis is parallel to the coiling axis. A, Projection over the front plane of a simple structure made up with four spheres. B, Projection of the same structure over the base plane.

chamber (proloculus) in a structure growing according to the two conditions of the model (i.e., according to the principle of isometry). A relationship between R_p and R_1 for the chambers after the first regular chamber can be established by equating equations (7) and (8):

$$R_1^3 = R_p^3 (Kt + 1)\delta_{FRC}/Kt. \quad (9)$$

In the following we will refer to R_1 as the effective initial radius. Although the discrepancy between R_p and R_1 is not important for comparing the effects of the different parameters on the shape of planktic foraminiferal shells, it should be considered when comparing the volumetric properties of the shells. In those instances, the effective initial radius must be used. Equation (9) provides the correction factor to calculate the effective radii of the chambers when using equation (7) instead of equation (5). It further follows from equation (9) that the effective initial radius can only be calculated when the δ_{FRC} is known.

The first sphere merely acts as a starting point in our model. Its size, as indicated by the radius, is a scaling factor. The role of the initial chamber in our simulation model may be equivalent to that of the proloculus, that of the two-chambered shell, or that of the three-chambered shell. However, since the proloculus differs from subsequently formed chambers in various aspects (Brummer et al. 1987), we prefer not to establish a definite relationship between the initial radius and specific stages of test formation. In conclusion, the size of the chambers is defined by one parameter Kt and one scaling factor R_1. Three additional parameters have to be introduced for locating the chambers in a three-dimensional space.

Position of the Chambers.—The position of any chamber is given by its center in a system of cylindrical coordinates. In log-spirally coiled shells, the centers of the successive spheres lie on a three-dimensional curve (fig. 3). The projection of this curve on a plane perpendicular to the coiling axis (the XZ plane in fig. 3) is a logarithmic spiral that can be described by the following equation in polar coordinates,

$$X(\Theta) = X_0 e^{b\Theta} \quad (10)$$

where $X(\Theta)$ is the radial distance from the coiling axis to a point placed at Θ radians from the origin of angles, b is a constant specifying the tightness of coiling, and X_0 is the distance from the first point in the curve to the coiling axis (fig. 3). In order to keep the effective shape of the chambers constant, the angle between centers of consecutive chambers measured in a plane perpendicular to the coiling axis must also be constant. This angle (ϕ) is the second parameter and equals 2π divided by the number of chambers per whorl. Thus, the position of the center of any chamber on the curve according to equation (10) is determined by

$$X_n^{+1} = X_0 e^{bn\phi}. \quad (11)$$

In the model, the size and the position of

the chambers are not independent from each other. If we define Kr as the ratio between consecutive chambers radii,

$$Kr = (Kt + 1)^{1/3}, \quad (12)$$

the following expression relates the rate of radius increase to the tightness of coiling and the number of chambers per whorl,

$$Kr = e^{b\phi}. \quad (13)$$

Thus, b needs not to be a new parameter of the model, but is a constant dependent on Kr and ϕ (cf. Signes et al. 1988).

The displacement of the chambers along the coiling axis (rate of translation) is determined by Ky, the third parameter, which is defined by the following equation,

$$\Delta Y/\Delta X = (Y_{n+1} - Y_n)/(X_{n+1} - X_n) = Ky, \quad (14)$$

where Y_n is the distance between the centers of the first and nth chamber measured along the coiling axis (fig. 3). When $Ky = 0$, the shell is planispiral.

The relative distance from the center of any chamber to the coiling axis, D, is the fourth and last parameter of the model. It is defined as the distance from the center of a chamber to the coiling axis divided by the radius of the chamber. The value of this parameter is constant for all chambers after the first regular chamber:

$$D = X_n/R_n. \quad (15)$$

When D equals one, all chambers are tangent to the coiling axis. If D is larger than one, an umbilicus results.

In addition to the initial radius, a second scaling factor is necessary to determine a structure, namely, the total number of spheres in the structure, N.

In summary, four parameters (Kt, ϕ, Ky, D) and two scaling factors (R_p, N) must be supplied to the program in order to simulate fully a foraminiferal shell. Although the chambers are represented by spheres in the above model, the conclusions of this study apply to shells with any chamber shape as long as the structures are isometric, that is, meet the two conditions of the model.

The Morphospace

By definition, the four parameters (Kt, ϕ, Ky, and D) are independent from each other in the model, and any different combination determines a different shell structure. All the possible combinations determine the morphological scope, or morphospace, of the model. According to chamber arrangement, four nonoverlapping regions may be defined:

1. Shells consisting of a set of isolated (unconnected) chambers. This is the region where the overlap, defined as the ratio of the radius of a chamber to the distance between its midpoint and the one of the succeeding chamber (Berger 1969), is smaller than $1/(Kr + 1)$. The other three regions are filled with constructions consisting of overlapping spheres which, however, do not necessarily occur in planktic foraminifers.

2. Shells made up of linearly arranged chambers (i.e., only consecutive chambers overlap each other). Uniserial shells result either when both D and ϕ are large, or when Ky is large and the number of chambers per whorl is one. Uniserial planktic foraminifers, however, do not exist.

3. Shells with completely involute chambers, so that every new chamber encloses the whole shell. These types emerge from all combinations of parameters that yield a chamber overlap (O-lap) value greater than $1/(Kr - 1)$ (see eq. 17). Involute arrangements are found in *P. obliquiloculata* but only the adult stage of *Orbulina universa* d'Orbigny is completely involute.

4. Shells with chambers arranged in a log-spiral mode. These types result from combinations of parameters intermediate between 2 and 3.

The region of the morphospace occupied by structures resembling planktic foraminifers is relatively small, probably because some morphologies are out of the scope of the developmental programs running in planktic foraminifera (they are impossible to construct whereas others are not compatible with the planktic way of life, i.e., they are unadaptive). Some morphologies, however, appear to be highly adaptive. Although most morphological patterns have arisen independently in each period of radiation, many homeomorphs

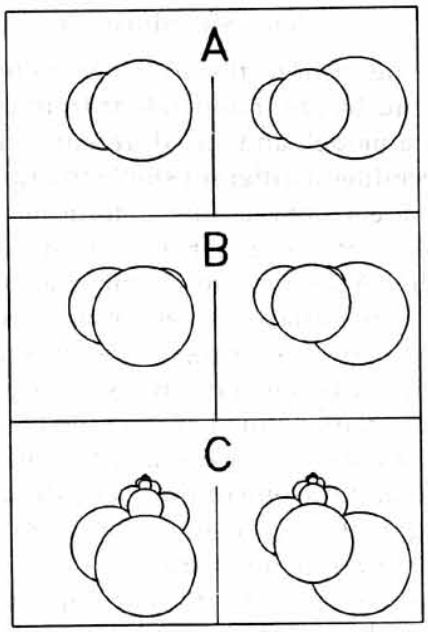

FIGURE 4. Axial views from the three perpendicular planes. Structures are shown in side (left) and frontal (right) view. *Ky* is varied (see table 1 for other parameters and variables). A, $Ky = 0$, planispiral. B, $Ky = 1$, low trochospiral. C, $Ky = 2$, high trochospiral.

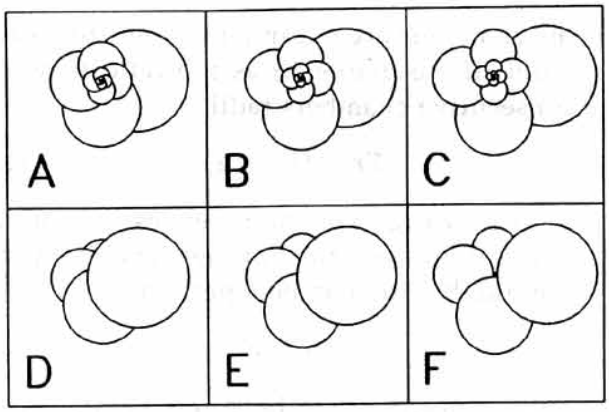

FIGURE 5. Spiral (A–C) and corresponding umbilical (D–F) views. A and D, $D = 0.8$; B and E, $D = 1$, all chambers are tangent to the coiling axis; C and F, $D = 1.2$, the umbilicus is open. See table 1 for other parameters.

have evolved (Norris 1991). This phenomenon, in which very similar shell morphologies develop in unrelated groups of planktic foraminifera, is called iterative homeomorphy (Cifelli 1969; Hart 1980). The "polyphyletic" origin of several lineages pointed out by several authors (Banner 1982; Kennett and Srinivasan 1983) may be a consequence of this phenomenon. The convergence may be so strong that it is difficult to distinguish between Neogene taxa and their Paleogene homeomorphs (e.g., *Subbotina linaperta-Globigerinoides sacculifer*; *Globorotalia* (*Turborotalia*) *centralis-Globorotalia* (*Turborotalia*) *inflata*).

The vast majority of modern planktic foraminiferal shells ranges between planispiral and high trochospiral (fig. 4). A nearly flat spiral side is typical of many species. In terms of our model, this means that most shells have values for the translation rate between 0 (planispiral) and a little more than 1 (slightly spiroconvex).

The umbilicus is a morphological feature widely used in taxonomy. In naturally occurring shells, chambers embrace the coiling axis or have a wide umbilicus (fig. 5). In terms of the model, the values of D vary between a little less than 1 or about 2. A very low value of D is found for the spherical stage of *O. universa*.

The number of chambers per whorl is another feature that differs among species and usually changes during ontogeny. Higher values are commonly found during early ontogeny, abruptly decreasing in later stages. The most important change occurs during the transition from the juvenile to the neanic stage (Parker 1962; Brummer et al. 1987). In general, the number of chambers per whorl normally varies between three and seven. In terms of the model, the angle between consecutive chambers ranges between $2\pi/3$ and $2\pi/7$ radians (fig. 6).

Whereas the absolute dimension of any chamber can be measured by its radius (fig. 7), the relative proportions of the chambers are measured by ratio between consecutive chamber radii. During normal development, every chamber is larger than the previous one (except for a variety of terminal chambers, such as kummerform ones). This sets the lower limit for the rate of radius increase higher than one. The most common values for this variable are between 1.1 and 1.3 even though higher values (ca. 3–4) may be recorded in certain ontogenetic stages such as for the terminal spherical chamber of *O. universa*. When the rate of radius increase equals 1.1, the volume of a new chamber is by definition one-third of the previous shell volume (see eqs. 1 and 12). When the rate of radius increase is 1.3, the volume of every new chamber is 1.2 times the previous shell volume (fig. 8). The

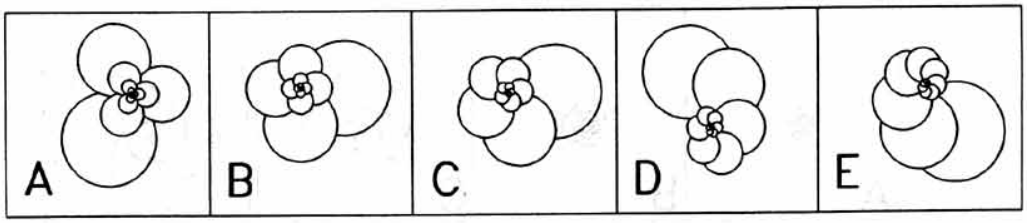

FIGURE 6. Spiral views of structures with varying number of chambers per whorl (C/W). A, 3 C/W; B, 4 C/W; C, 5 C/W; D, 6 C/W; E, 7 C/W. See table 1 for the other parameters.

rate of radius increase in combination with the number of chambers per whorl determines the lobateness of the shell. A high value for the rate of radius increase in combination with a low number of chambers per whorl produces "lobate" structures. In contrast, a low value for the rate of radius increase in combination with a large number of chambers per whorl gives rise to a more rounded outline in spiral or umbilical views.

Stereometric Properties of Shell Architectures

The shell volume provides a first-order measure for the biomass and may be secondarily related to the size of the food items or to amount of food needed. The outer surface area (*OSA*) is defined as the surface area, at each growth stage of the shell, which is in contact with the environment. The surface area available for exchange between the cytoplasm and the outer environment (gases, nutrients etc.) is only secondarily related to the outer surface area because it also depends on the porosity. By analogy to benthic rotaliid foraminifers, we assume that the exchange of gases takes place through the pores (Berthold et al. 1976; Leutenegger and Hansen 1979). The respiration rate may thus also be perceived as a derivative of the outer surface area.

The calcification process of planktic foraminifers was described with the so-called bilamellar calcification model (Reiss 1957). This model conjectures that both the outside and the inside of a new chamber are calcified. The new calcite layers not only cover the new chamber but also extend over earlier chambers. The new calcite layer extends over a maximum of about four chambers on the inside and over a maximum of roughly two chambers on the outside. The thickness of the inner layer is approximately one-fourth of the outer one. On both sides the new calcite layer tapers toward the earlier chambers. Because of the complexity of the calcification process and because of individual variation, it is difficult to assess the total amount of calcite that has been secreted at a certain stage. For first approximation, we assume that the total amount of calcite that has been secreted is *related* to the total surface area (*TSA*). The total surface area is defined as the sum of the outer surface area from the initial chamber to the one under consideration:

$$TSA_n = \sum_{i=1}^{n} OSA_i.$$

Both the volume and surface area of the geometric structures were determined with a computer program. As it is extremely difficult to calculate the volumes and surface areas of these complex structures by numerical analysis, we have developed a new method to estimate these variables (Ott et al. 1992). The memory of a personal computer is configured as a cube with an edge length of 150 bytes (1200 bits). The structure under study is defined within this "bitspace." It is scaled up or down to fit in the cube as close as possible. The bits inside and outside the structure are

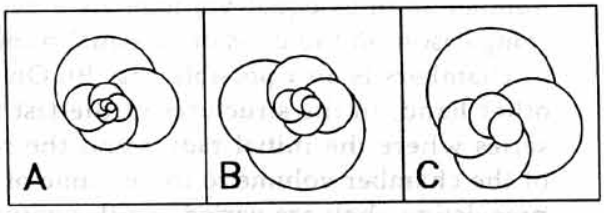

FIGURE 7. Spiral views of three structures differing in "prolocular size." The ratio of their initial radii are approximately 1:2:4. A, R_p = 2.4; B, R_p = 4.7; C, R_p = 9.5. See table 1 for the other parameters. In order to keep the same scale as in figures 4–8, fewer chambers have been drawn for B and C.

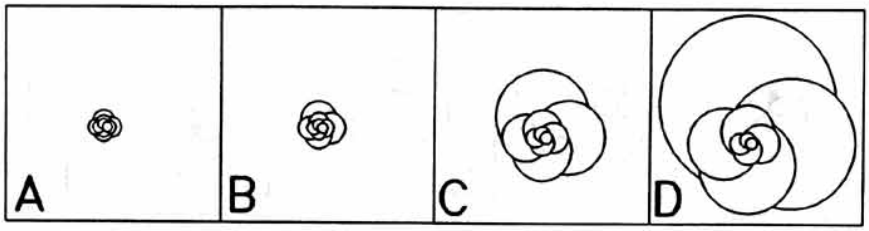

FIGURE 8. Spiral view of structures with values of Kt increasing from 0.3 to 1.5. A, $Kt = 0.3$; B, $Kt = 0.5$; C, $Kt \approx 1$; D, $Kt \approx 1.5$. See table 1 for the other parameters.

assigned 1 and 0 respectively. Scanning the cube bitwise, the 1's are added up to estimate the volume and the number of transformations between 0 and 1 are added up to estimate the surface area. The volume estimations in turn allow the calculation of the δ_{FRC} (see Appendix A). From equation (9) the effective radius may then be calculated. A scaling factor derived from the discrepancy between the effective initial radius (R_1) and the initial radius supplied to the computer (R_p) is used to correct for the radii that fit the model. This method provides estimates for the shell volume and the outer surface area with relative errors smaller than 2% and 5%, respectively.

In order to know how the volume, the outer surface area, and the total surface area of the structures are affected by the parameters of the model, 70 structures grouped into five series have been studied (table 1; figs. 4–8). All these structures are within the region of the morphospace corresponding to modern planktic foraminiferal morphologies. Within each series, only one parameter is varied. Comparison of the structures within and between the five series are made on the basis of equal volume (biomass). As the parameters that affect volume (R_p and Kt) are kept constant in the first three series, equal chamber number implies equal volume. As a result, comparison on the basis of an equal number of chambers is also possible (fig. 9). On the other hand, in the structures of the last two series where the initial radius and the ratio of the chamber volume to the volume of the preexisting shell are varied, similar volumes are reached at different chamber numbers (fig. 10).

The data for volumes and surfaces of the five series of structures are summarized in figures 9 and 10. The results have been scaled down to the same effective initial radius except in the fourth series where the effect of its variation is studied. Only the chambers after the FRC are compared. In these examples, the FRC is the ninth chamber; that is, the discussion is restricted to chambers 9 through 21.

In the first series, the values of the translation rate are such that the structures range from planispiral to high trochospiral (table 1; fig. 4). The increase in the OSA going from planispiral ($Ky = 0$) to low trochospiral (flat spiral side; $Ky = 1$) is insignificant (<1%). For a translation rate larger than one, the outer surface area changes more drastically. A high trochospiral structure ($Ky = 2$) has about 14% more outer surface area than the former two. These variations, however, are small in comparison to the increase in the outer surface area with size. As a consequence of definition, the total surface area and the ratios of outer surface area to shell volume and total surface area to shell volume vary in the same proportion as the outer surface area (fig. 9J–M).

In the second series, the relative distance to the coiling axis (D) is varied between 0.8 and 1.2 (table 1). This corresponds to a shift from a nonumbilical structure to a more evolute structure with an open umbilicus (fig. 5). In the second structure all chambers are tangent to the coiling axis ($D = 1$) and the outer surface area is 8% larger than in the first structure where $D = 0.8$. For values of D larger than one, the outer surface area changes more drastically. The structure where $D = 1.2$ has 25% more outer surface area than that where $D = 0.8$. The variations between the structures are rather small compared to the increase of the outer surface area with size (fig. 9E–H). The proportionality is the same for the total

TABLE 1. Data for the structures drawn in figures 1–7. The first two rows list the scaling factors (total number of chambers and the initial radius) that are supplied to the computer. The subsequent four rows contain the values for the parameters of the model. The next four rows list the number of chambers per whorl (Ch/Whorl), the ratio between radii of consecutive chambers after the first regular chamber (FRC) (*Kr*), the *O*-lap for an equivalent structure determined according to the model of Berger (1969), and the whorl expansion rate (*W*) for an equivalent structure determined according to the model of Raup (1966). The last three rows labeled R_1, δ_{FRC}, and FRC correspond to the effective initial radius, the ratio between the volume of any chamber after the FRC to that of a complete sphere with the same radius, and the number of the FRC. In the first three columns, the translation rate is varied. In the next three columns, the relative distance from the center of any chamber to the coiling axis is varied. In the next five columns, the number of chambers per whorl is varied. The next series consists of three columns in which the initial radius is varied, and in the last four columns, the rate of radius increase is varied.

	Ky			*D*								R_r			*Kt*			
	0	1	2	0.8	1.0	1.2	3C/W	4C/W	5C/W	6C/W	7C/W	2.4	4.7	9.5	0.3	0.5	≈1.0	≈1.5
Chambers	21	21	21	21	21	21	21	21	21	21	21	21	21	21	21	21	21	21
R_r	2	2	2	2	2	2	2	2	2	2	2	2	4	8	2	2	2	2
ϕ	1.57	1.57	1.57	1.57	1.57	1.57	2.09	1.57	1.26	1.05	0.90	1.57	1.57	1.57	1.57	1.57	1.57	1.57
Kt	1.20	1.20	1.20	1.20	1.20	1.20	1.20	1.20	1.20	1.20	1.20	1.20	1.20	1.20	0.30	0.50	0.95	1.46
D	1	1	1	0.8	1	1.2	1	1	1	1	1	1	1	1	1	1	1	1
Ky	0	1	2	1	1	1	1	1	1	1	1	1	1	1	1	1	1	1
Ch/Whorl	4	4	4	4	4	4	3	4	5	6	7	4	4	4	4	4	4	4
Kr	1.3	1.3	1.3	1.3	1.3	1.3	1.3	1.3	1.3	1.3	1.3	1.3	1.3	1.3	1.091	1.145	1.25	1.35
O-lap	0.61	0.6	0.57	0.75	0.6	0.5	0.5	0.6	0.71	0.82	0.93	0.6	0.6	0.6	0.67	0.65	0.62	0.58
W	2.86	2.86	2.86	2.86	2.86	2.86	2.19	2.86	3.72	4.84	6.26	2.86	2.86	2.86	1.42	1.72	2.44	3.32
R_1	2.3	2.4	2.4	2.3	2.4	2.4	2.4	2.4	2.3	2.3	2.2	2.4	4.7	9.5	2.7	2.6	2.4	2.3
δ_{FRC}	0.87	0.90	0.94	0.79	0.90	0.95	0.90	0.90	0.85	0.80	0.76	0.90	0.90	0.90	0.58	0.73	0.86	0.91
FRC	5	6	2	10	6	5	7	6	6	7	7	6	6	6	18	13	6	5

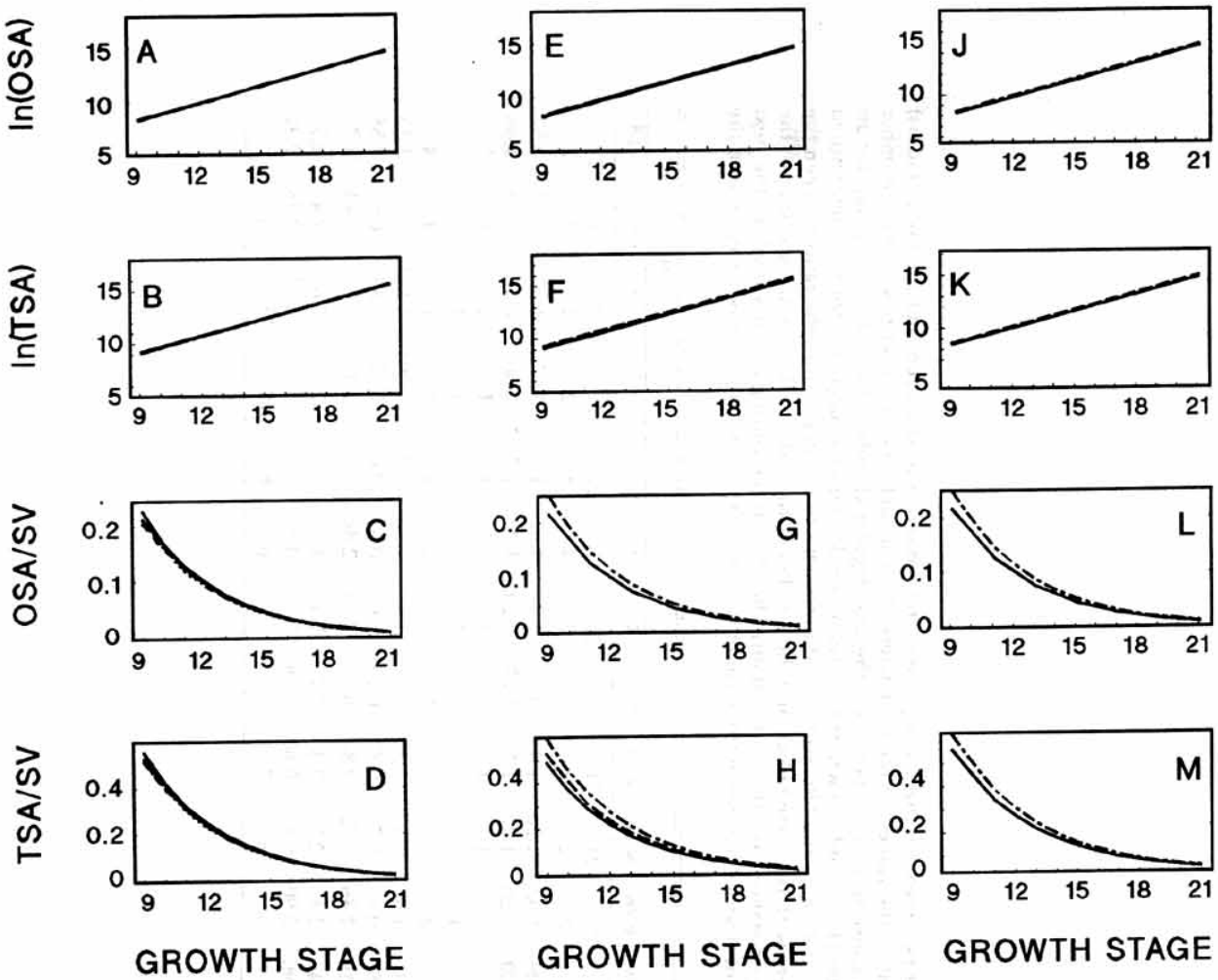

FIGURE 9. Outer surface area (*OSA*), total surface area (*TSA*) and both relative to shell volume (*SV*) as a function of chamber number. A–D, Data for five structures differing in the number of chambers per whorl. E–H, Data for three structures differing in *D*; J–M, Data for three structures differing in trochospirality. See text for further explanation.

surface area, the outer surface area per shell volume, and the total surface area per shell volume.

In the third series, ϕ is progressing from values corresponding to three to seven chambers per whorl (table 1; fig. 6). The outer surface area decreases very little with an increase in the number of chambers per whorl (fig. 9A–D). At equivalent stages of growth, a structure with seven chambers per whorl has 6% less outer surface area than a structure with only three chambers per whorl. Note that these changes are small in comparison with the increase of outer surface area with size, that is, from one chamber to the other. Therefore, the relationships between the outer surface area and the chamber number of the five structures are very similar and appear as one (fig. 9A–D). The total surface area and the ratios of outer surface area to shell volume and total surface area to volume decrease proportionally.

In the fourth series, the initial radius (R_p) is varied from 2.4 to 4.7 to 9.5, the approximate proportions are 1:2:4 respectively (table 1; fig. 7). Because this is a scaling factor affecting size, an increase in the initial radius implies that the same size or equivalent volume is reached at an earlier chamber number (fig. 10A–E). Since this parameter does not affect shell morphology, a doubling of the the initial radius leads to an increase of the surface area by a factor of four and to an increase of the volume by a factor of eight at equiv-

alent chamber increments. If the structures in this series are compared at stages of equivalent shell volume, there are neither differences in the outer surface area nor in the total surface area. These relationships have been used in all other series in order to establish comparisons between structures having the same effective initial radius.

In the fifth series, the ratio between the chamber volume to the volume of the preexisting shell (Kt) is varied between 0.3 and 1.5 (table 1). This parameter is the most important one controlling size. Contrary to the initial radius, Kt affects both size and shell morphology. For instance, the lobateness increases (fig. 8). A small increase in Kt produces an exponential rise in shell volume and in the total surface area (fig. 10F–K). Comparisons between the structures are made on the basis of equal volume. Although the outer surface area is not appreciably affected by a change in Kt, the total surface area is. For instance, in the second, third, and fourth structure of this series, a very similar volume is reached at the twenty-first, thirteenth, and tenth chambers, respectively, whereas the outer surface area remains constant as does the ratio between outer surface area and shell volume. The total surface area at the tenth chamber of the fourth structure is, however, 90% smaller than in the second structure with 21 chambers. In other words, for a given shell volume, the total surface area decreases with increasing Kt. The explanation is, that with lower Kt more chambers are needed to attain a certain size, and therefore, the equation for the total surface area contains more terms.

The effects of the parameters on surface area, volume, and derived properties may be summarized as follows. The outer surface area and the total surface area and their ratios to shell volume vary little with the number of chambers per whorl, the relative distance from the center of the chamber to the coiling axis, or the displacement of the chambers along the coiling axis. The variation in the outer surface area and in the total surface area between two consecutive chamber increments is greater than the difference measured at the same chamber number (equal size) between

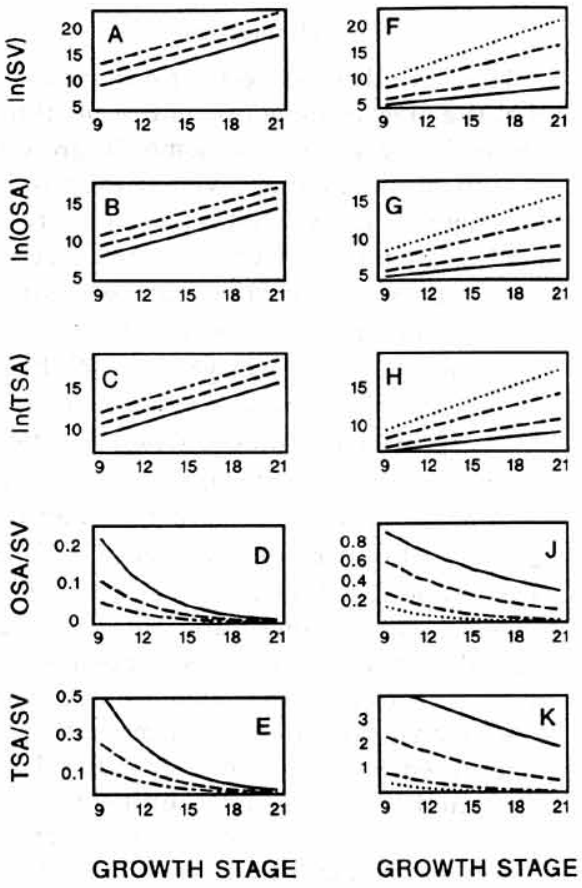

FIGURE 10. Shell volume, outer surface area, total surface area and the latter two relative to shell volume as a function of chamber number. A–E represent data of three structures differing in the size of their initial spheres: solid line, $R_i = 2.4$; long-dashed line, $R_i = 4.7$; long- and short-dashed line, $R_i = 9.5$. F–K represent data of four structures differing in Kt: solid line, $Kt = 0.3$; long-dashed line, $Kt = 0.5$; long- and short-dashed line, $Kt = 0.95$; dotted line, $Kt = 1.46$. See the text for further explanation.

structures with different shell morphologies (fig. 9A,B,E,F,J,K). The influence of size is most important at later ontogenetic stages.

With respect to the parameters that directly affect size (i.e., the initial radius and the ratio between the volumes of consecutive chambers), the variation in the surface area, volume and derived ratios is more pronounced. In any case, the variation decreases with increasing size (figs. 9, 10). Size by itself is the most important factor controlling the variation in the outer surface area and the total surface area and their ratios to the shell volume.

Discussion

The central hypothesis of our approach is that the laws of development in planktic foraminifera give rise to isometric growth. It should be noted that, even if each isolated ontogenetic growth phase is isometric, the shell as a whole may be allometric. Yet, isometry is the most important feature of our model. At this point, it is important to define what is meant by isometric growth. Within the framework of the model proposed herein, isometric growth is achieved when the effective chamber shape is constant and the volumes of consecutive chambers are in geometric progression. In terms of Bookstein (1989), size-free shape variables and shape-free size variables do not change after the first regular chamber. Because it seems impossible to determine the effective chamber shape in actual specimens, the external chamber shape has been used in morphometric studies. Because the shell walls are not infinitisimally thin, wall thickness increases with increasing chamber size, and because of the bilamellar calcification mode, isometric growth may be obscured.

According to Olsson (1971, 1972, 1973) and Wei et al. (MS) some planktic foraminifers grow allometrically. Olsson used the logarithmic spiral for shape description in several species of *Globorotalia*. Three variables were recorded for each specimen in spiral view: the maximum width of the chamber, the chamber radius (defined as the maximum distance from the coiling axis to the edge of the chamber), and the angle of rotation. The latter variable is equivalent to ϕ in our model. Chamber width and chamber radius were converted to a logarithmic scale, plotted first as a function of the accumulated angle of rotation and then against each other. A linear regression analysis was performed for each of the three pairs of variables. In most cases the data closely fitted to one straight line or more because of ontogenetic variation. Although the slopes in the plots of the logarithm of chamber radius versus the logarithm of chamber width were always very close to one, Olsson qualified foraminiferal shells as allometric.

Wei et al. measured 20 linear distances between reference points defined at two orientations of *G. inflata*. Sheared principal-component analysis suggested that this species grows allometrically, that is, that shape varies with test size.

These conclusions represent a challenge to our conception of foraminiferal morphology. Geometric patterns of coiling arise as a consequence of a characteristic mode of growth. Log-spiral patterns of coiling are explained as a result of exponential growth per chamber increment while keeping chamber shape constant. Because chamber size determines chamber position, in log-spirally coiled shells, we expect the slope of the regression of the logarithm of chamber radius versus the logarithm of chamber width to be one.

Several comments may be made with respect to the procedure followed by Olsson and Wei et al. (1) All measurements were taken from specimens where the outline of early chambers is blurred by multiple layers of calcite (see figs. in Olsson 1971, 1972, 1973; plate 2 in Wei et al. MS; cf. Brummer et al. 1987; Plate I-1a,b). True chamber shape variations during ontogeny and apparent chamber shape changes caused by later calcification also influence the measurement. Thus, data from early chambers are less reliable than those from later ones. (2) During ontogeny, planktic foraminiferal morphology may change rather drastically (Parker 1962; Olsson 1971, 1972, 1973; Brummer et al. 1986, 1987, Wei et al. MS). Uniform spiral coiling may thus be confined to ontogenetic stages rather than to the shell as a whole. Consequently, the value of the parameters that determine size and position of the chambers may not be the same for all chambers. (3) Olsson's regression lines may not be significantly different from 1, as neither standard errors, confidence intervals nor tests for comparison of the slopes are reported. These considerations show that deviation from 1 may be an artifact. As his graphs are nevertheless very close to 1, his results can also be interpreted in favor of isometric growth. Malmgren and Kennett (1976) studied the biometry of *Globigerina bulloides* d'Orbigny and concluded that it grows isometrically.

TABLE 2. Relationships between the parameters of the model presented here (REMAKER) and those of the models of Raup (1966) and Berger (1969). A continuous line indicates equivalence; a dashed line indicates that both parameters have similar roles but are differently defined. "Implicit" means that the parameter can be derived from parameters of the current model. See the text for further explanation.

Raup 1966		REMAKER		Berger 1969
S		none		none
D	– – – – –	D		implicit
T	———	Ky		none
W		implicit (b)		implicit
None		ϕ	———	A-angle
None		Kt	– – – – –	Q-ratio
None		implicit		O-lap

Comparison with Other "Fixed-Axis" Models.—There are important affinities between the model presented here and the models of Raup (1966) and Berger (1969). First of all, they deal with log-spirally coiling and isometric structures. The model of Raup (1966) was designed to simulate the basic shape of accretionary shells, like those of gastropods, cephalopods, pelecypods, and brachiopods. The model of Berger (1969) and the one presented here have been designed to simulate discrete shell growth, typically that of planktic foraminifera. The relationships between the parameters of the three models serve as a basis for their comparison (table 2).

In our model, the parameter D is defined in a slightly different way than its homonym in the model of Raup (1966). He defined this parameter as the relative distance from the generating curve to the coiling axis. D is 0 when the chambers are tangent to the coiling axis. The equivalent situation in our model arises when D equals 1. The displacement of the chamber centers along the coiling axis (Ky) is equivalent to the whorl translation rate (T) of Raup. The whorl expansion rate (W) of Raup controls the coiling around the axis and relates to b in our model according to the following equation (derived from equations 11 and 13):

$$W = e^{2\pi b} \quad \text{or} \quad b = \ln W/2\pi. \quad (16)$$

There is no parameter equivalent to Raup's shape of the generating curve (S) in our model or in Berger's. In the latter models, chamber shape is constant and spherical.

Berger (1969) did not explicitly mention that his model generated isometric structures. Thus, he probably chose his parameters because of their frequent usage in micropaleontological terminology, rather than because of their affinity with isometric growth. He used the chamber radius increase, the number of chambers per whorl, and the overlap between successive chambers as parameters for his model. Because he did not use a parameter for the whorl translation rate, his model is restricted to handle planispiral structures. Because isometry was not his main consideration, he did not account for the difference between the initial radius (R_p) and the effective initial radius (R_1), nor did he compensate for the different relative losses of volume caused by overlap in early chambers, that is, the early stages of his model do not grow exponentially.

Three parameters define his model; the A-angle and the angle ϕ are the same but the first is given in degrees and the second in radians. The Q-ratio is exactly the same as Kr and O-lap can be expressed in terms of our model as follows:

$$O\text{-lap} = [D \cos \alpha(Kr^2 - 2Kr \cos \phi + 1)^{1/2}]^{-1}, \quad (17)$$

where α is the angle between a plane perpendicular to the coiling axis and the line connecting the centers of two successive chambers. In planispiral structures α equals 0. This angle can also be expressed in terms of our model as

$$\alpha = \operatorname{cotg}[Ky(Kr - 1)] \div [(Kr^2 - 2Kr \cos \phi + 1)^{1/2}]. \quad (18)$$

Conversely, the parameter D of our model can be expressed in terms of the parameters of the model of Berger as

$$D = [O\text{-lap}(Q^2 - 2Q \cos A + 1)^{1/2}]^{-1} \quad (19)$$

where Q is the Q-ratio and A is the A-angle.

A characteristic feature of Berger's model is that the first chamber in every structure is forced to be tangent to the coiling axis. This causes a deviation of early chambers from the logarithmic spiral and, consequently, a discrepancy between the position of these chambers and the chambers in an analogous structure determined with our model. In other words, if we restrict ourselves to planispiral coiling, it is possible to determine nearly the same structures with both models. The only difference is the position of some of the early chambers; these seldom exceed the first regular chamber. With respect to the volume and surface area calculations, our method (Ott et al. 1992) enables more accurate estimates.

Functional Significance.—The functional significance of different morphological traits of foraminiferal shells has received much attention (see, e.g., Marszalek et al. 1969; Hottinger 1984, 1986; Hemleben et al. 1989; De Renzi 1988). In a series of papers, Brasier (1982, 1986) emphasized the role of the apertures in the history of foraminiferal shell architectures as they determine the lines of communication between the organism and the environment. Herein, we take a complementary approach. We focus on general shell morphology and its relationship with the outer surface area, the total surface area, and shell volume because these may have played or still play a major role in the evolution of these organisms. These magnitudes change exponentially with size and have important consequences on physiology and functional requirements. In combination with the porosity, the outer surface area may govern the maximal rate of gas exchange and may thus be connected to the respiration rate. The volume (biomass), on the other hand, is related not only to the amount of oxygen needed but also to the amount of prey needed. The total amount of calcite secreted is directly related to the total surface area. The latter is thus proportional to shell weight. In a second order relationship, the total surface area per unit of volume is proportional to shell density and thus to buoyancy (a relationship also anticipated by the modeling of Brasier 1986). Because of its relationship to the total amount of calcite in the shell, the total surface area is an indicator of the calcification effort. The calcification effort must be expressed per unit of volume because the calcium pool is probably biomass dependent (Anderson and Faber 1984). The calcification effort may be expressed per chamber or for the whole shell. We define the total calcification effort as the ratio between the total surface area and the shell volume, and calcification effort per increment as the ratio between the outer surface area of chamber n and the shell volume (OSA_n/SV). A high total calcification effort implies that more calcification matrix has to be produced and that more energy is required for calcium-pump activity. Thus, energetic arguments may counteract development toward a high total calcification effort. The size of the calcium pool, on the other hand, may limit the calcification effort per increment. Usually, if the calcification effort per increment is small, the total calcification effort is large. For instance, the general trend in planktic foraminiferal ontogeny and phylogeny seems to be from a low to a high calcification effort per increment and from a high to a low total calcification.

Our model indicates that shell size is the major factor that determines the value of the ratio of surface area to biomass and the ratio of total surface area to biomass. Only changes in the initial radius (R_p) and in the ratio between chamber volume and the existing shell volume (Kt) are shown to have a significant effect on the ratio between the outer surface area and the shell volume and on the ratio between the total surface area and the shell volume. Changes in the initial radius do not alter shell morphology. Thus, changes of shell morphology, other than the one caused by Kt, only provide a fine tune-up of these ratios, mostly in the early stages of development. During these early stages of development, however, changes in the shell morphology as a result of the other parameters may be relatively important. For example, increases in D and Ky may compensate for the lowering in the ratio of the outer surface area to the shell volume and of the total surface area to

the shell volume between consecutive chamber increments.

An increase in the initial radius or in *Kt* leads to a reduction in the number of chambers before a given size or volume is reached (fig. 10). However, only the increase of *Kt* will reduce the total calcification effort. These observations stress the possible role of size as a controlling factor during foraminiferal ontogeny and phylogeny. The drastic morphological changes between consecutive stages during ontogeny are also size-dependent (Brummer et al. 1986, 1987).

Isometric development imposes restrictions on the organism's strategy for chamber arrangement, which are related to scaling. Spherical chambers have the lowest possible outer surface area to volume ratio. If the disparate increase in volume respective to outer surface area limits the growth of planktic foraminifers, shells with a large outer surface area to volume ratio will be favored, that is, small, highly spired shells with few chambers per whorl. Examples of this strategy are the biserial form *Streptochilus globigerus* (Schwager) and the triserial form *Gallitellia vivans* (Cushman). They are small and can be regarded as extremely high trochospiral shells with only two and three chambers per whorl, respectively. A large ratio of outer surface area to shell volume also seems to characterize specimens at the base of the adaptive radiations. The Middle Jurassic species *Globuligerina bathoniana* (Pazdrowa) is small and has three to four chambers per whorl arranged in a high trochospiral (Riegraf 1987). Early Tertiary planktic foraminifers, on the other hand, are also small but have more chambers per whorl and are low trochospiral. Some, however, have a large umbilicus that also increases the outer surface area to shell volume ratio (e.g., *Eoglobigerina eobulloides*). Apparently, at this size, the ratio of the outer surface area to the shell volume does not restrict the development of features that tend to increase the ratio. The transition from the juvenile to the adult stage, which is generally marked by a reduction of the number of chambers per whorl and an increase in trochospiralness, may be controlled by the ratio of the outer surface area to the shell volume.

Deviations from isometry would provide a solution to size constraints and would allow the organism to attain larger sizes and possibly enhance the reproductive capacity. Our model does not allow deviations from isometry. However, the same two conditions that explain log-spiral coiling after the first regular chamber also explain the deviation from log-spiral coiling before the first regular chamber. To maintain exponential growth (keep *Kt* constant) before the first regular chamber in structures with spherical chambers, two alternatives were proposed: (1) to maintain a log-spiral throughout ontogeny, or (2) keep *Kr* constant. The first solution implies that the chamber radii are not in geometric progression; that is, *Kr* is not constant before the first regular chamber. This consequence makes the first solution very unlikely, because log-spiral coiling is achieved as a consequence of a constant *Kt*. As shown earlier, the second solution demands modifications of at least one of the three following parameters, ϕ, *Ky*, or *D*. Therefore, before the first regular chamber, the number of chambers per whorl must be higher, the structure must be lower trochospiral or the umbilicus must be larger than after the first regular chamber. These adaptations or a combination thereof imply that the chambers before the first regular chamber deviate from a log-spiral pattern of coiling. Neither of the two solutions has mathematical priority. Which solution, however, is realized in planktic foraminifera? Many juvenile stages of planktic foraminifers are characterized by a higher number of chambers per whorl, flatter coiling, and a more open umbilicus than neanic or adult stages (Parker 1962; Brummer et al. 1987). These observations fit remarkably with the second solution. Although additional testing is required, these data support our initial assumption that isometry is an important trait of planktic foraminiferal ontogeny. It would suggest that the laws of growth behind planktic foraminiferal architecture are oriented toward the maintainance of exponential growth per chamber increment. Together with a constant effective chamber shape, this gives rise to isometric shells, if not for the shell as a whole, then at least for each onto-

genetic stage. Their ontogeny may be tentatively explained as follows. The chamber radii of each ontogenetic stage are in geometric progression and only the centers of juvenile chambers deviate from the log-spiral. Apparently, the first neanic chamber is equivalent to the first regular chamber. Thus, from the neanic stage onward, log-spiral coiling and exponential growth per stage do not exclude each other and isometric growth occurs. In this context, the drastic morphological changes during the neanic stage may be viewed as a constructional bridge between juvenile and adult architecture. In other words, the neanic stage marks the transition from a set of "juvenile" parameters to "adult" ones while maintaining exponential growth per chamber increment.

The size constraints caused by metabolic limitation may have played a preeminent role in the evolution and the diversification at the species level (Brasier 1982, 1986). In planktic foraminifers, the biomass determines the number of gametes that can be produced. Morphological changes occuring in later ontogenetic stages, such as the transition from neanic to adult or from adult to terminal, may have first appeared in the course of the evolution after developmental solutions allowed the organism to attain bigger sizes. Changes in chamber shape may be such a solution to overcome the limits imposed by size. In our model, the chamber shape is kept spherical throughout ontogeny. In planktic foraminifers, however, chamber shape is not constant during growth. Embryonic chambers tend to be spherical, whereas the juvenile chambers range from spherical to subspherical or ovoid (Sverdlove and Bé 1985; Brummer et al. 1987). The most prominent changes in chamber shape occur in the adult stages of some large species such as, for example, the development of "clavate" chambers in *Globigerina digitata*, and an involute globular chamber in *Orbulina universa*. The secretion of kummerform and saclike chambers in *G. sacculifer* is probably related to the reproduction process and has little to do with size or growth problems (Bijma et al. 1990; Bijma and Hemleben MS).

Future investigations should focus on the transformation of the shape parameters during ontogenetic development and during the evolution lineages, especially at the beginning of the adaptive radiations.

Conclusions

We argued that very elementary laws of construction may give rise to a *Bauplan* that leads to growth according to the principle of geometric similitude. Thus, isometry may play a key role in the macroevolutionary patterns of planktic foraminifers. Because this hypothesis cannot be directly tested, a computer simulation was performed. Exponential growth per stage and log-spiral coiling could be the most prominent characters of development in planktic foraminifera. We have reached the following conclusions.

1. The demonstration of isometry in planktic foraminifera needs further empirical testing from real life histories.
2. In terms of the model, the neanic stage of Brummer (1986, 1987) is equivalent to the first regular chamber, and the drastic morphological changes from the juvenile to the adult stage might represent the necessary transition from one set of parameters defining juvenile architecture to the other set that determines the adult shell configuration.
3. Thus, uniform coiling may be confined to ontogenetic stages, rather than to the shell as a whole; that is, the shell as a whole may be allometric.
4. Size is the major factor determining the values of the ratios of surface area to biomass and the total calcification effort to biomass.
5. Of the parameters tested, only the proportionality between consecutive chamber volumes (Kt) may influence the surface area to biomass ratio and the total calcification effort per unit of biomass to a large extent.
6. The other shape parameters only provide a fine tune-up of these ratios, mostly in the early stages of development.
7. The above conclusions are not only valid for structures that have spherical chambers, but for any chamber shape as long as growth is determined by the two basic conditions of the model; that is, growth is isometric.

Acknowledgments

We are grateful to V. Caselles (University of València) and P. Charissiadis (University of Tübingen) for many discussions about

methods to calculate volume and surface area of complex structures. W. H. Berger (Scripps), G.-J.A. Brummer (Free University of Amsterdam), R. K. Olsson (Rutgers University), M. De Renzi (University of València), M. Brasier (University of Hull), K.-Y. Wei (Yale University), G. Vermeij (University of California), and an unknown reviewer are acknowledged for valuable comments on various versions of the manuscript. This work has been supported by the Comisión Asesora de Investigación Científica y Técnica (nr. 2934/83.C2), the Deutscher Akademischer Austausch-Dienst (nr. 313/025/030/7) and the Conselleria de Cultura (Generalitat Valenciana) and by Deutsche Forschungsgemeinschaft (He/697/3).

Literature Cited

Ackerly, S. C. 1989. The kinematics of accretionary shell growth, with examples from brachiopods and molluscs. Paleobiology 15:147–164.

Anderson, O. R., and W. W. Faber, Jr. 1984. An estimation of calcium carbonate deposition rate in a planktonic foraminifer *Globigerinoides sacculifer* using ^{45}Ca as a tracer: a recommended procedure for improved accuracy. Journal of Foraminiferal Research 14:303–308.

Banner, F. T. 1982. A classification and introduction to the Globigerinacea. Pp. 142–239 *in* F. T. Banner and A. R. Lord, eds. Aspects of micropaleontology. Allen and Unwin, London.

Berger, W. H. 1969. Planktonic foraminifera: basic morphology and ecologic implications. Journal of Paleontology 43:1369–1383.

Berthold, W. U., H. Gocht, Ch. Hemleben, and H. Netzel. 1976. Cytologische und Ökologische Aspecte der Morphogenese und Struktur rezenter und fossiler Protisten-Skelette. Zentralblatt für Geologie und Paläontologie 2:325–338.

Bijma, J., J. Erez, and Ch. Hemleben. 1990. Lunar and semilunar reproductive cycles in some spinose planktonic foraminifers. Journal of Foraminiferal Research 20:117–127.

Bonner, J. T. 1982. Evolution and development. Springer, Berlin.

Bookstein, F. L. 1986. Size and shape spaces for landmark data in two dimensions. Statistical Science 1:181–242.

———. 1989. "Size and shape": a comment on semantics. Systematic Zoology 38:173–180.

Bookstein, F. L., B. Chernoff, R. Elder, J. Humphries, G. Smith, and R. Strauss. 1985. Morphometrics in evolutionary biology. Special Publication 15. Academy of Natural Science of Philadelphia, Philadelphia.

Brasier, M. D. 1982. Architecture and evolution of the foraminiferid test: a theoretical approach. Pp. 1-41 *in* F. T. Banner and A. R. Lord, eds. Aspects of micropaleontology. Allen and Unwin, London.

———. 1986. Form, function and evolution in benthic and planktic foraminiferid test architecture. Pp. 251–268 *in* B. Leadbeater and R. Riding, eds. Biomineralization in lower plants and animals. Clarendon, Oxford.

Brummer, G.J.A., Ch. Hemleben, and M. Spindler. 1986. Planktonic foraminiferal ontogeny and new perspectives for micropaleontology. Nature (London) 319:50–52.

———. 1987. Ontogeny of extant spinose planktonic foraminifera (*Globigerinidae*): a concept exemplified by *Globigerinoides sacculifer* and *G. ruber*. Marine Micropaleontology 12:357–381.

Cifelli, R. 1969. Radiation of Cenozoic planktonic foraminifera. Systematic Zoology 18:154–168.

De Renzi, M. 1982. La forma orgànica: un pretext per a establir contacte amb alguns problemes de fons de la biologia. Pp. 351–388 *in* Estudios dedicados a Juan Peset Aleixandre. Universidad de Valencia, Valencia.

———. 1988. Shell coiling in some larger foraminifera: general comments and problems. Paleobiology 14:387–400.

Gould, S. J. 1966. Allometry and size in ontogeny and phylogeny. Biological Reviews of the Cambridge Philosophical Society 41:587–640.

———. 1968. Ontogeny and the explanation of form: an allometric analysis. *In* D. B. Macurda, ed. Paleobiological aspects of growth and development, a symposium. Paleontological Society Memoirs 2. Journal of Paleontology 42:81–98(suppl.).

———. 1970. Evolutionary paleontology and the science of form. Earth-Science Reviews 6:77–119.

———. 1988. Trends as changes in variance: a new slant on progress and directionality in evolution. Journal of Paleontology 62:319–329.

Hart, M. B. 1980. A water depth model for the evolution of the planktonic Foraminiferida. Nature (London) 286:252–254.

Healy-Williams, N., and D. F. Williams. 1981. Fourier analysis of test shape of planktonic foraminifera. Nature (London) 289: 485–487.

Hemleben, Ch., M. Spindler, and O. R. Anderson. 1989. Modern planktonic foraminifera. Springer, New York.

Hickman, C. S. 1980. Gastropod radulae and the assessment of form in evolutionary paleontology. Paleobiology 6:276–294.

Hottinger, L. 1984. Foraminifères de grande taille: signification des structures complexes de la coquille. Pp. 309–315 *in* Benthos'83; 2nd International Symposium on Benthic Foraminifera (Pau, April 1983), Pau and Bordeaux, March 1983.

———. 1986. Construction, structure and function of foraminiferal shells. Pp. 219–235 *in* B. Leadbeater and R. Riding, eds. Biomineralisation in lower plants and animals. Clarendon, Oxford.

Huber, B. T. 1987. Ontogenetic morphometrics of some Upper Cretaceous foraminifera from the southern high latitudes. Antarctic Journal of the United States 22(5):15–17.

Kennett, J. P., and M. S. Srinivasan. 1983. Neogene planktonic foraminifera: a phylogenetic atlas. Hutchinson Ross, Stroudsburg, Pa.

Lebreton, J. D., and C. Millier. 1982. Modèles dynamiques déterministes en biologie. Masson, Paris.

Leutenegger, S., and H. J. Hansen. 1979. Ultrastructure radiotracer studies of pore function in foraminifera. Marine Biology 54:11–16.

Lohmann, P. 1983. Eigenshape analysis of microfossils: a general morphometric procedure for describing changes in shape. Mathematical Geology 15:659–672.

Macleod, N., and J. A. Kitchell. 1990. Morphometrics and evolutionary inference: a case study involving ontogenetic and developmental aspects of evolution. Pp. 283–299 *in* F. J. Rohlf and F. L. Bookstein, eds. Proceedings of the Michigan Morphometrics Workshop. Museum of Zoology. Special Publication 2, The University of Michigan.

Malmgren, B. A., and J. P. Kennett. 1976. Biometric analysis of phenotypic variation in recent *Globigerina bulloides* d'Orbigny in the southern Indian Ocean. Marine Micropaleontology 1:3–25.

Marszalek, D. S., R. L. Wright, and W. W. Hay. 1969. Function of the test in Foraminifera. Transactions of the Gulf Coast Association of Geological Societies 19:341–352.

Moseley, H. 1938. On the geometric form of turbinate and discoid shells. Philosophical Transactions of the Royal Society, London 128:351–370.

Norris, R. D. 1991. Biased extinction and evolutionary trends. Paleobiology 17:388–399.

Okamoto, T. 1988. Analysis of heteromorph ammonoids by differential geometry. Palaeontology 31:35–52.

Olsson, R. K. 1971. The logarithmic spire in planktonic foraminifera: its use in taxonomy, evolution, and paleoecology. Transactions of the Gulf Coast Association of Geological Societies 21:419–432.

———. 1972. Growth changes in the *Globorotalia fohsi* lineage. Eclogae Geologica Helveltica 65:165–184.

———. 1973. Growth studies on *Globorotalia exilis* Blow and *Globorotalia pertenius* Beard in the hole 154A section, leg 15, Deep Sea Drilling Project. Initial Reports of the Deep Sea Drilling Project XV 14:617–624.

Ott, R., M. Signes, J. Bijma, and Ch. Hemleben. 1992. A computer method for estimating volumes and surface areas of complex structures consisting of overlapping spheres. Mathematical and Computer Modeling.

Parker, F. L. 1962. Planktonic foraminiferal species in Pacific sediments. Micropaleontology 8:219–254.

Raup, D. M. 1966. Geometric analysis of shell coiling: general problems. Journal of Paleontology 40:1178–1190.

———. 1972. Approaches to morphologic analysis. Pp. 28–45 *in* T.J.M. Schopf, ed. Models in paleobiology. Freeman, Cooper, San Francisco.

Raup, D. M., and A. Michelson. 1965. Theoretical morphology of the coiled shell. Science (Washington, D.C.) 147:1294–1295.

Reiss, Z. 1957. The Bilamellidea, nov. superfam., and remarks on Cretaceous globorotaliids. Cushman Foundation of Foraminiferal Research, Contributions 8:127–145.

Riegraf, W. 1987. Planktonic foraminifera (Globuligerinidae) from the Callovian (Middle Jurassic) of Southwest Germany. Journal of Foraminiferal Research 17:190–211.

Rohlf, F. J. 1990. Morphometrics. Annual Review of Ecology and Systematics 21:299–316.

Rohlf, F. J., and F. L. Bookstein, eds. 1990. Proceedings of the Michigan Morphometrics Workshop. Museum of Zoology. Special Publication 2, The University of Michigan.

Scott, G. H. 1970. Basal Miocene correlation: *Globigerinoides* from southern New Zealand. Micropaleontology 16:385–398.

———. 1972. The relationship between the Miocene Foraminiferida *Globorotaliamiozea* and *G. praemenardii*. Micropaleontology 18:81–93.

———. 1973. Ontogeny and shape in *Globorotalia menardii*. Journal of Foraminiferal Research 3:142–146.

———. 1974. Biometry of the foraminiferal shell. Pp. 55–151 *in* R. H. Hedley and C. G. Adams, eds. Foraminifera 1. Academic Press, London.

Seilacher, A. 1970. Arbeitskonzept zur Konstruktions-Morphologie. Lethaia 3:393–396.

Signes, M., M. De Renzi, and L. Marquez. 1988. A study of spiral coiling in Operculina. Revue de Paléobiologie 2:885–893.

Stanley, S. M. 1973. An explanation for Cope's rule. Evolution 27:1–26.

Sverdlove, M. S., and A.W.H. Bé. 1985. Taxonomic and ecological significance of embryonic and juvenile planktonic foraminifera. Journal of Foraminiferal Research 15:235–241.

Tabachnick, R. E., and F. L. Bookstein. 1990a. The structure of individual variation in Miocene *Globorotalia*. Evolution 44:416–434.

———. 1990b. Resolving factors of landmark deformation: Miocene *Globorotalia*, DSDP site 593. Pp. 269–281 *in* F. J. Rohlf and F. L. Bookstein, eds. Proceedings of the Michigan Morphometrics Workshop. Museum of Zoology. Special Publication 2, The University of Michigan.

Tappan, H., and A. R. Loeblich, Jr. 1988. Foraminiferal evolution, diversification and extinction. Journal of Paleontology 62:695–714.

Thom, R. 1977. Stabilité structurelle et morphogénèse. Inter Editions, Paris.

Thompson, D'A. W. 1942. On growth and form, 2d ed. Reprinted in 1972. Cambridge University Press, Cambridge.

Waddington, C. H. 1968. Towards a theoretical biology. 1. Prolegonema. IUBS symposium. University Press, Edinburgh.

Appendix A

The following volumetric relationships apply to any structure that is in agreement with the two hypotheses of our model. Because the model largely eliminates chamber shape the relationships apply to any isometric structure independent of the shape of the chambers (as long as the effective shape of the chambers is constant).

No.	Chamber volume	Shell volume
1	$CV_1 = CV_1$	$SV_1 = CV_1$
2	$CV_2 = Kt\ SV_1$	$SV_2 = SV_1 + CV_2 = SV_1(Kt + 1)$
3	$CV_3 = Kt\ SV_2 = Kt\ SV_1 = CV_2(Kt + 1)$	$SV_3 = SV_2 + CV_3 = SV_1(Kt + 1)^2$
4	$CV_4 = Kt\ SV_3 = CV_2(Kt + 1)^2$	$SV_4 = SV_3 + CV_4 = SV_1(Kt + 1)^3$
n	$CV_n = Kt\ SV_{n-1} = CV_2(Kt + 1)^{n-2}$	$SV_n = SV_{n-1} + CV_n = SV_1(Kt + 1)^{n-1}$

In a further step, chamber shape may be introduced. Here, chambers are spherical.

No.	Chamber volume	Chamber radius
1	$CV_1 = cR_1^3$	
2	$CV_2 = cR_2^3\delta_2 = Kt\ CV_1$	$R_2^3 = Kt(1/\delta_2)R_1^3$
3	$CV_3 = cR_3^3\delta_3 = (Kt + 1)CV_2$	$R_3^3 = (Kt + 1)(\delta_2/\delta_3)R_2^3$
4	$CV_4 = cR_4^3\delta_4 = (Kt + 1)CV_3$	$R_4^3 = (Kt + 1)(\delta_3/\delta_4)R_3^3$
m	$CV_m = cR_m^3\delta_m = (Kt + 1)CV_{m-1}$	$R_m^3 = (Kt + 1)(\delta_{m-1}/\delta_m)R_{m-1}^3$
$m + 1$	$CV_{m+1} = cR_{m+1}^3\delta_m = (Kt + 1)CV_m$	$R_{m+1}^3 = (Kt + 1)(\delta_m/\delta_m)R_m^3 = (Kt + 1)R_m^3$
n	$CV_n = cR_n^3\delta_m = (Kt + 1)CV_{n-1}$	$R_n^3 = (Kt + 1)R_{n-1}^3$

Where, $c = 4\pi/3$ and the $m + 1$th chamber is the FRC. The $\delta(i)$ factor is defined as the ratio between chamber volume (i.e., the effective volume added to the shell by a chamber) and the volume of a sphere with the same radius. Consequently, equation (5) may be derived: $R_n^3 = Kt(Kt + 1)^{n-2}\ R_n^3/\delta_n$. This applies to all chambers.

Appendix B

List of parameters and scaling factors of the geometric model and abbreviations in alphabetical order.

- b A constant specifying the tightness of coiling
- CV_n Volume of nth chamber
- D Distance of the chamber center to the coiling axis divided by the radius of this chamber (related to umbilicus)
- δ Ratio between the volume of the chamber and that of a complete sphere with the same radius
- δ_{1R} Ratio between the volume of any chamber after the first regular one and the volume of a complete sphere with the same radius
- Kr Ratio between consecutive chambers radii
- Kt Ratio between a chamber volume to the volume of the preexisting shell (relates to exponential growth)
- Ky Expresses the displacement of the chambers along the coiling axis (related to trochospirality)
- OSA_n Outer surface area of the shell after secretion of the nth chamber
- R_n Radius of the nth chamber
- R_0 Initial radius
- R_1 Effective initial radius
- SV_n Shell volume after secretion of the nth chamber
- TSA_n Total surface area; addition of the outer surface areas of the first to the nth chamber
- ϕ Angle between consecutive chambers (related to the number of chambers per whorl)
- $X(\Theta)$ Radial distance from the coiling axis to a point placed at Θ radians from the origin of angles
- X_n Distance from the first point in the curve to the coiling axis
- X_n Distance from the center of the nth chamber to the coiling axis
- Y_n Distance between the centers of the first and nth chamber measured along the coiling axis